PCCP

ROYAL SOCIETY OF CHEMISTRY

PAPER

View Article Online
View Journal | View Issue

Cite this: *Phys. Chem. Chem. Phys.*, 2025, **27**, 24404

Janus nanoparticles with decyls on one side direct extended cell membrane anchoring

Puja Garai, Ilora Maiti and Nikhil R. Jana *

Received 10th July 2025,
Accepted 21st October 2025

DOI: 10.1039/d5cp02633d

rsc.li/pccp

One-side functionalization of nanoparticles can produce Janus structures with unique physical properties that direct differential interaction with biological interfaces compared with conventional nanoparticles. Here, we show that the functionalization of hydrophobic molecules on one side of the nanoparticle surface enhances the particle–particle interactions that decrease their colloidal stability in water but direct extended anchoring with the cell membrane. In particular, we synthesized 50–60 nm colloidal silica that comprises a porous silica core doped with gold/iron oxide nanoparticles and terminated with hydrophilic dextran groups on one side and with hydrophobic decyl groups on the other side. We show that this Janus structure induces nanoparticle-nanoparticle interactions *via* decyl groups that decrease their colloidal stability and drive attachment to the lipophilic cell membrane. A comparative study shows that these Janus nanoparticles can label the cell membrane faster than their respective symmetric nanoparticles and remain at the cell membrane for a longer time. These Janus nanoparticles can be used for magnetic cell separation without cytotoxicity and for drug delivery without the entry of the nanocarrier into the cell.

Introduction

A Janus nanoparticle with two different surface chemistries in a single particle offers unique physicochemical properties.[1,2] They can behave like a surfactant due to nanoscale asymmetry in hydrophilicity/hydrophobicity and offer extended cell surface attachment,[3,4] incomplete endocytic uptake,[3] membrane disruption properties[5,6] and enhanced antibacterial activities.[7,8] In addition, the Janus structure of particles can be used to make nano-/micro-motors with directional properties/movements that are useful for different applications, such as inhibiting amyloid fibrillation,[9] bacterial biofilm disruption,[10] delivering drugs to the tumor site[11] and ultrasound-based therapy.[12] Despite their unique properties, most of the reported Janus nanoparticles are >100 nm in size (SI, Table S1). This is due to the synthetic challenge and the difficulty in the characterization of Janus structures with sizes <100 nm.[2] Moreover, the physicochemical properties of Janus nanoparticles in the size range of 10–100 nm and the impact of Janus structures in biomedical applications are largely unexplored. In particular, the colloidal properties of Janus nanoparticles are not correlated with cellular interactions, although there are reports on the poor colloidal stability of Janus structures, along with extended cell surface attachment or enhanced membrane disruption property.[3,8]

It is known that the hydrophobic–hydrophilic balance plays a key role in cell-nanoparticle interactions as well as in the colloidal stability of nanoparticles, and the appropriate adjustment of hydrophobicity is important for efficient cell labeling over nanoparticle precipitation. We designed colloidal functional nanoparticles and nanodrugs of 10–50 nm size for cell delivery/therapy application.[13] In particular, we designed hydrophobic molecule-conjugated amphiphilic nanoparticles for enhanced interaction with the cell membrane,[14,15] lipid raft-mediated cell uptake *via* modular interaction with the cell membrane[14,15] and direct membrane penetration-based cell uptake that bypasses endocytosis.[16] We showed that covalent or electrostatic attachments of a hydrophobic molecule can influence endocytosis or direct membrane penetration-based cell uptake mechanism.[16] These results suggest that the control of hydrophobic–hydrophilic balance at the nanoparticle surface has an enormous impact on cell-nanoparticle interactions. Here, we show that Janus nanoparticles with covalently attached hydrophobic molecules on one side are colloidally less stable compared with the isotropic conjugation of the same hydrophobic molecule, and this property influences their interaction with the cell membrane. We show that the Janus structure induces nanoparticle-nanoparticle interactions using their hydrophobic groups and drives attachment to the lipophilic cell membrane. This stronger binding interaction leads to faster cell labeling and extended cell membrane attachment without the entry into the cytosol.

School of Materials Science, Indian Association for the Cultivation of Science, 2A & 2B Raja S. C. Mullick Road, Kolkata-700032, India.
E-mail: camnrj@iacs.res.in

Experimental procedure

Materials

Tetraethylorthosilicate (TEOS), [3-(2-aminoethylamino)propyl]trime thoxysilane (AEAPS), tetramethylammonium hydroxide (25 wt%) (TMAH), octadecylamine, methyl morpholin *N*-oxide, octadecene, glutaraldehyde solution, decylamine, dextran (MW-6000 Da), fluorescamine, sodium dodecyl sulfate (SDS), sodium cyano-borohydride ($NaCNBH_3$) and Dulbecco's modified Eagle's medium (DMEM) were purchased from Sigma-Aldrich. Cetyltrimethylammonium bromide (CTAB) and *N*,*N*,*N*′,*N*′-tetramethylethylenediamine were purchased from Alfa Aesar. Ammonia (25 wt%) was purchased from Merck. 3-(4,5-Dimethylthiazol-2-yl)-2,5-diphenyltetrazolium bromide (MTT) was purchased from Himedia.

Synthesis of nanoparticle-incorporated porous silica particles

Synthesis is carried out using our previously reported method.[17] In brief, 2 mL of thin silica-coated hydrophilic iron oxide was taken in a 250 mL beaker. Then, 45 mL of distilled water and 5 mL of 0.015 M CTAB solution were added under stirring conditions. After 15 min of stirring, 1.5 mL of 25% NH_3 solution was added to this solution. Next, 0.5 mL of an ethanolic solution of tetraethyl orthosilicate (300 μL dissolved in 2.5 mL ethanol), 2 mL of an ethanolic solution of AEAPS (50 μL of AEAPS dissolved in 10 mL of ethanol) and 2 mL of DMF were added stepwise at 5 min intervals. The whole solution was kept under stirring conditions for 3 h. Subsequently, excess ethanol was added for the precipitation of the particles. Next, the particles were isolated by centrifugation and washed three times with ethanol and three times with water. For removing CTAB, the particles were dispersed in an ethanolic solution of NH_4NO_3 (250 mg of NH_4NO_3 dissolved in 25 mL of ethanol) by sonication and the whole solution was heated to 80 °C for 1 h under stirring conditions. The process was repeated three times, and finally, the particles were dispersed in 5 mL of water and stored for further use.

Preparation of silica particle-stabilized wax microparticles

A silica particle-stabilized wax-water emulsion was prepared by following the reported method.[18] In a typical process, 20 mg of nanoparticle-incorporated silica particles was dispersed in 15 mL of water under magnetic stirring conditions. Then, the temperature was increased to 75 °C and at that temperature, 1 g of wax was added. After that, 1 mg of sodium dodecyl sulfate (SDS) was added to the above solution. The resulting mixture was stirred for 10 min and then cooled to room temperature, yielding solid wax microparticles with silica particles attached to the surface. These wax microparticles were then filtered, washed with water several times and dried under vacuum for 24 h. By this process, we obtained 600–700 mg of particles in each batch.

Preparation of Janus nanoparticles

Solid wax microparticles were used for functionalization with dextran by cyanoborohydride-based conjugation chemistry.[19] Briefly, 600 mg of wax microparticles was dispersed in 5 mL of water, and the pH was adjusted to 9 by adding *N*,*N*,*N*′,*N*′-tetramethyl ethylenediamine (TMEDA). Next, 6 mg of dextran was dissolved separately in 500 μL water and mixed with the above solution, followed by the addition of $NaCNBH_3$ solution (18 mg dissolved in 200 μL of water), and the solution was kept under magnetic stirring for 6 h. Next, the solid particles were isolated from the mixture by filtration and washed several times with water to remove excess dextran. Next, the solid particles were treated with cyclohexane-chloroform and sonicated for wax dissolution. The silica particles were then dispersed in 2 mL of a water-ethanol mixture and used for decylamine functionalization.

Decyl functionalization of silica particles was performed using decylamine *via* glutaraldehyde-based conjugation chemistry. In brief, 10 μL of glutaraldehyde was dissolved in 250 μL of ethanol and 20 μL of decylamine was separately dissolved in 250 μL of ethanol. Next, the two solutions were mixed, stirred for 30 min, and then the whole mixture was added to dextran-functionalized silica particles (2 mL) with continued stirring. After 30 min, 25 mg $NaCNBH_3$ was added and the stirring was continued for 6 h. The resulting particles were isolated by centrifugation, washed twice with ethanol and twice with water to remove excess glutaraldehyde/decylamine and finally dissolved in 1 mL of water (about 1 mg mL^{-1}) for further use.

Preparation of control nanoparticles

We have synthesized three different isotropically functionalized silica nanoparticle-terminated dextran (control a), low-density decyls (control) and high-density decyls (control b) starting from primary amine-terminated silica particles. Control a nanoparticles were prepared by following the reported method.[18] In brief, 20 mg of primary amine-terminated silica particles were dispersed in 10 mL of water and mixed with dextran solution (6 mg dextran dissolved in 500 μL water) and $NaCNBH_3$ solution (18 mg $NaCNBH_3$ dissolved in 200 μL water) and stirred for 6 h. After that, the solution was centrifuged and purified twice with water. Finally, the particles were dissolved in water for future application.

For the preparation of control, 5 mg of primary amine-terminated silica particles were dispersed in 1 mL of a water-ethanol mixture. In a separate vial, glutaraldehyde solution (10 μL glutaraldehyde dissolved in 250 μL ethanol) and decylamine solution (20 μL decylamine dissolved in 250 μL ethanol) were prepared and after 30 min of mixing, the solution was added to the 1 mL nanoparticle dispersion under magnetic stirring. After 30 min, $NaCNBH_3$ solution (25 mg dissolved in 200 μL water) was added and stirring was continued for 6 h. Then, the prepared particles were isolated by centrifugation and washed twice with ethanol and water, respectively. The resultant control particles were dispersed in water. For the preparation of control b, all procedures were the same as those for control, except that the glutaraldehyde-decylamine conjugate was added in 10 μL increments with 5-minute intervals until all the solution was added.

Estimation of primary amine

The fluorescamine-based titration method was used to quantify the primary amines present in Janus particles as well as in control particles.[20] First, the fluorescamine test was performed using glycine as a standard in the range of 20–400 μM. Typically, 100 μL of glycine solution was added to 800 μL of borate buffer solution of pH 9. Then, 100 μL of an acetone solution of fluorescamine (1×10^{-2} M) was mixed, and the fluorescence was measured at 493 nm (by exciting at 400 nm). A linear calibration curve was obtained by plotting fluorescence intensity with respect to glycine concentration. The linear equation was obtained as follows: $Y = 9.29 \times 10^{-4} X - 63.62$ with $R^2 = 0.99$ (Y is the glycine concentration in μM and X is the fluorescence intensity). Similarly, the fluorescamine test was performed for Janus particles and isotropic control particles. The fluorescence intensity was measured at 493 nm, and using the calibration curve described above, the primary amines present were estimated.

Cell labelling study

We have used the CHO cell in our study. CHO is a Chinese hamster ovary cell that is commonly used as a model cell for *in vitro* studies. For the cell labelling study, we have conjugated the nanoparticles with fluorescein using NHS-fluorescein. Cells were cultured in DMEM medium with 10% heat-activated fetal bovine serum (FBS) and 1% penicillin–streptomycin at 37 °C and 5% CO_2 atmosphere. Next, the cells were cultured overnight in a 24-well plate with 500 μL of DMEM, and then 70 μL of particle dispersion was added, followed by 4–8 h of incubation. After incubation, the cells were washed with PBS buffer solution and the washed cells were used for imaging studies or further incubated in a fresh medium for 8–24 h for long-term localization studies.

Cell viability assay

For the cell viability study, CHO cells were cultured in 24-well plates in cell culture media. After that, the cells were treated with different doses of particles for 24 h and then washed with PBS buffer and fresh DMEM medium was added. Next, 50 μL of freshly prepared MTT solution (5 mg MTT in 1 mL deionized water) was added to each well and incubated for 4 h. Next, the supernatant was removed carefully, leaving formazan in the plate and dissolved in a sodium dodecyl sulfate (SDS) solution (8 g of SDS dissolved in 40 mL of DMF–H_2O mixture). Finally, absorbance was measured at 570 nm. Cell viability was estimated assuming 100% viability for cells treated without the particles.

Results and discussion

Janus nanoparticles with dextran on one side and decyls on the other side *via* the Pickering microemulsion approach

The Pickering microemulsion approach was used for the synthesis of Janus nanoparticles[20] (Fig. 1). Pickering microemulsion consists of liquid droplets stabilized by solid particles, rather

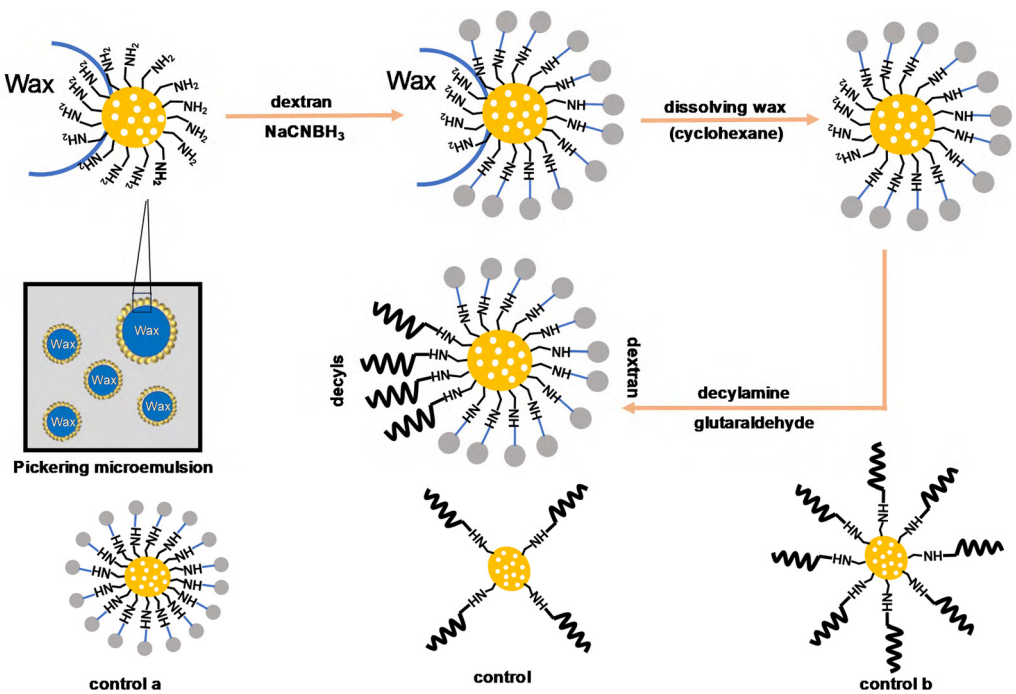

Fig. 1 Schematic representation of the synthesis of Janus nanoparticle *via* the one side attachment of decyl groups. First, the Pickering microemulsion is prepared using primary amine-terminated silica particles as the stabilizer. At this stage, the wax side of the primary amines of silica particles is blocked, and the rest of the outside amines are conjugated with dextran. Next, the wax is removed to uncover the amine groups on the other side and conjugated with decylamine. Isotropic functionalization of dextran (control a) and decylamine (control and control b) is performed in the absence of Pickering microemulsion to generate different control nanoparticles.

than traditional surfactants.[20] In the present case, silica nanoparticle-stabilized wax microdroplets are used as a Pickering microemulsion. First, porous silica nanoparticles doped with Au/iron oxide nanoparticles with an average size of 60 nm are prepared using our reported method[17] (Fig. 2a). These nanoparticles are terminated with primary amines that can be used for conjugation chemistry. These nanoparticles are used as a stabilizer for the Pickering microemulsion of wax. Typically, solid wax is mixed with an aqueous dispersion of silica nanoparticles and heated at 75 °C to convert it into liquid wax. Under stirring conditions, liquid wax is converted into microdroplet-terminated silica particles as a stabilizer. Next, the mixture is cooled to room temperature, giving rise to solid wax microparticles with silica particles attached to their surfaces. At this stage, the wax side of the primary amines of silica particles is blocked, and the rest of the outside amines are conjugated with dextran. Evidence of accessibility of one side of silica nanoparticles, when present as a Pickering microemulsion stabilizer, has been investigated *via* electron microscopy. When incubated with anionic gold nanoparticles (20 nm), followed by the removal of wax, it has been found that 20 nm gold nanoparticles are attached only to one side of the silica particle (Fig. 2b). This one side attachment suggests that the wax side of primary amines is not accessible for the reaction and that dextran functionalization occurs only on the other side. The control experiment shows that if colloidal silica particles are incubated with anionic gold nanoparticles (20 nm), the gold nanoparticles are randomly attached to all sides of the silica particles (SI, Fig. S1). After functionalizing with dextran, wax is removed to uncover the amine groups on the other side and decyl functionalization is then performed *via* glutaraldehyde-based conjugation with decylamine. Control nanoparticles were prepared *via* isotropic functionalization of dextran (control a) or decylamine (control and control b) in the absence of Pickering microemulsion.

Primary amines present at the silica nanoparticle surface were estimated at each step of the conjugation chemistry *via* the fluorescamine test.[21] Results show that colloidal silica nanoparticles of 2.0 mg mL^{-1} have an amine concentration of 1.16 mM that becomes 380 μM after dextran conjugation on one side and is further lowered to 20 μM for the Janus nanoparticle (SI, Fig. S2). Similarly, the control nanoparticle with isotropically conjugated decylamine has a concentration of 50 μM. This decrease in primary amine concentration at each step suggests that they are reacting with dextran and decylamines. Moreover, these findings indirectly suggest that the number of decyls in the control particle is about 3 times that in the Janus nanoparticle. The control b nanoparticle also has isotropically conjugated decylamine, but with a higher density, which decreases water solubility and increases nanoparticle agglomeration.

Fig. 2a shows a representative TEM image of Au nanoparticle-doped silica particles at two different magnifications primarily used for this study. The average size of the particles is 50–60 nm. The hydrodynamic size of the particles was determined using dynamic light scattering measurements. Both Janus nanoparticles and control nanoparticles show relatively larger sizes in the 50–300 nm range due to their aggregation tendency (Fig. 3a). However, the size of the Janus nanoparticle appears larger (100–400 nm) compared to the size of the control nanoparticles (50–300 nm). This result suggests that Janus nanoparticles have a greater tendency to aggregate. Janus nanoparticles exhibit a low positive charge as indicated by the zeta potential, and a similar positive charge is also

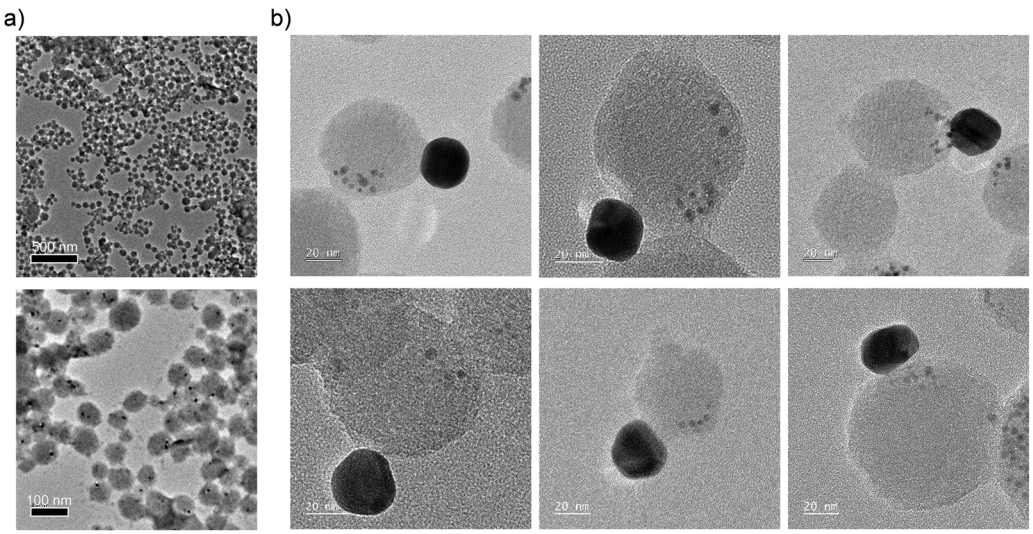

Fig. 2 (a) TEM images of Au nanoparticle-doped silica particles that are primarily used for this study at two different magnifications. (b) Evidence of one side accessibility of silica particles when present as a microemulsion stabilizer and identification of the Janus structure *via* electron microscopy. Small gold nanoparticle (3–5 nm)-doped silica particles are used as the stabilizer for wax microemulsion and incubated with anionic gold nanoparticles (20 nm), and then, the wax is removed. TEM images show that 20 nm gold nanoparticles are attached to the one side of the silica particles.

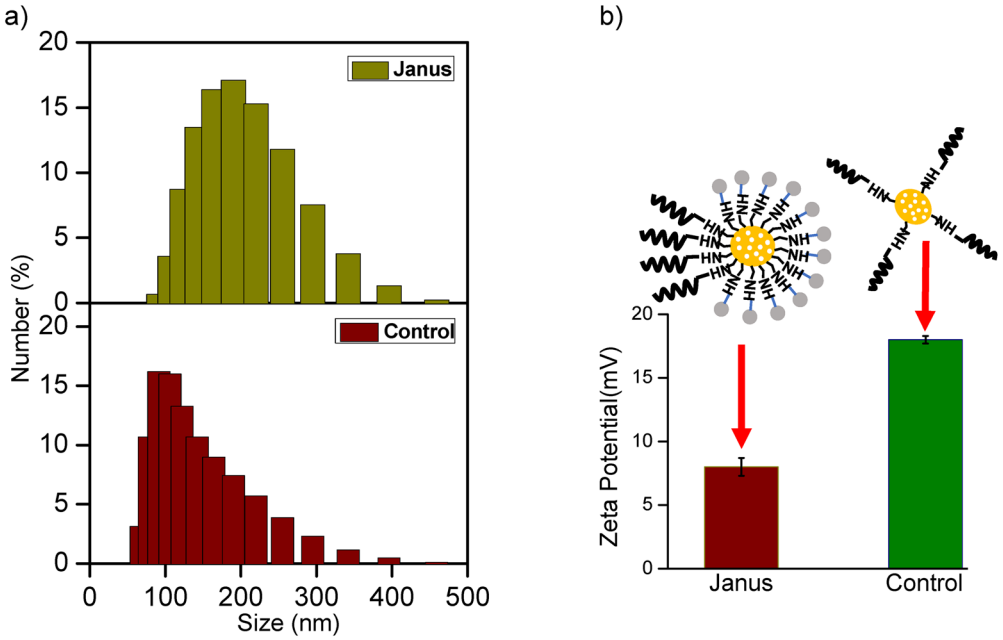

Fig. 3 (a) Typical hydrodynamic size of Janus nanoparticles *vs.* control nanoparticles with isotropic decyl functionalization. (b) Zeta potential of Janus nanoparticles compared with the control nanoparticles with isotropic decyl functionalization. Error bars are the average of 3 independent experiments.

observed for the control nanoparticles (Fig. 3b). Such a positive charge arises from the remaining primary amine groups, which yield a cationic charge *via* protonation.

Lower colloidal stability of Janus nanoparticles

We have extensively investigated the colloidal properties of Janus silica nanoparticles and compared them with those of control silica nanoparticles. Colloidal nanoparticles are prepared in water or ethanol, and their dispersion stability is then studied with respect to time. It is observed that Janus nanoparticles start precipitating after 2 h in both water and ethanol (Fig. 4). In contrast, control nanoparticles remain dispersed for up to 24 h. This result clearly suggests lower colloidal stability of Janus nanoparticles. We further investigated the colloidal

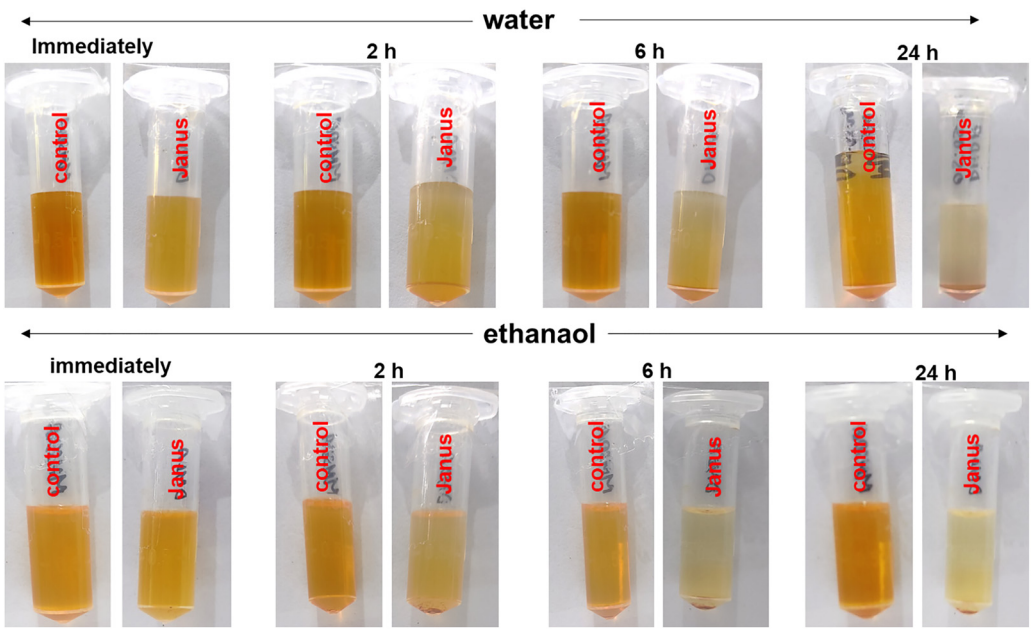

Fig. 4 Evidence of lower colloidal stability of Janus nanoparticles as compared with control nanoparticles with isotropic decyl functionalization. Colloidal nanoparticles are prepared in water or ethanol at 1.0 mg mL^{-1} and digital images are captured for up to 24 h, showing that Janus nanoparticles begin to precipitate after 2 h.

stability of control b particles in water with more decyls at the surface. The results indicate that the particles begin to precipitate within an hour (SI, Fig. S3).

The solvent-dependent particle–particle interaction of control b nanoparticles is further studied *via* DLS size measurements in DMSO-water mixtures of varied volume percentages and compared with that of Janus nanoparticles. Results show that the colloidal stability of control b nanoparticles decreases with increasing water content, as evident from the increased hydrodynamic size. However, Janus nanoparticles precipitate after 2 h for all the tested DMSO-water mixture systems (SI, Fig. S4). These results suggest that particle–particle interactions are solvent-independent for Janus nanoparticles. We have further studied particle aggregation of Janus nanoparticles *via* SEM imaging. Dilute solutions were used for sample preparation in order to avoid drying-induced particle aggregation. Results show that Janus nanoparticles form smaller assemblies of 4–20 nanoparticles (SI, Fig. S5). Considering the presence of hydrophobic decyl groups at the particle surface, particle–particle interactions are expected for both Janus and control nanoparticles. Moreover, considering the presence of 3 times more decyl groups, more aggregation is expected in the control nanoparticles. However, we have observed more aggregation in Janus nanoparticles. This has been reflected in a higher hydrodynamic size for Janus than the control (Fig. 3a) and increased precipitation of Janus nanoparticles. This is because the presence of decyl groups on one side of the Janus nanoparticle offers surfactant-like properties that induce particle–particle interactions (similar to micelle formation *via* surfactant assembly). SEM imaging of aggregates further revealed a 3D network for control b nanoparticles, whereas control nanoparticles showed relatively fewer network structures (SI, Fig. S6).

Extended cell membrane attachment of Janus nanoparticles

We have investigated the consequences of this lower colloidal stability of Janus nanoparticles in their interaction with the biological interface. We selected live cells for this interaction study as the cells have a lipophilic membrane for interactions, and cell-nanoparticle interactions are key for biomedical applications of Janus nanoparticles. Typically, cells are incubated with nanoparticles for different time periods and then the washed cells are used for imaging under bright field or fluorescence mode and the merged images are shown here. Nanoparticles are conjugated with fluorescein for their tracking under a fluorescence microscope. We used freshly prepared colloidal nanoparticles for cell labelling experiments in order to ensure the Janus nanoparticles remained well-dispersed. Under these conditions, the particles can attach to the cell membrane primarily through hydrophobic interactions.

Two important results were identified. First, Janus nanoparticles label cells faster than control nanoparticles. For example, Janus nanoparticles can label cells within 4 h compared to the 8 h required for control nanoparticles (Fig. 5). Second is the extended attachment of Janus nanoparticles at the cell membrane without entry into the cytosol. For example, Janus nanoparticles can stay at the membrane for 24 hours (Fig. 5, 6 and SI, Fig. S7, S8). In contrast, control nanoparticles can significantly enter the cytosol. These results clearly suggest enhanced membrane attachment of Janus nanoparticles compared to control nanoparticles with isotropic functionalization of decyl groups. Additional experiments show that control a nanoparticles have very poor cell labeling properties and control b nanoparticles precipitate in the culture media, which restrict their cell labelling properties.

The cell uptake mechanism has been studied in the presence of different endocytosis inhibitors and under different conditions. Results show that nanoparticle labeling is not stopped either at 4 °C or in the presence of sucrose, suggesting endocytic uptake is not involved (SI, Fig. S9 and S10). We further investigated the application potential of Janus nanoparticles with their extended cell membrane attachment properties. We found that the extended cell membrane attachment

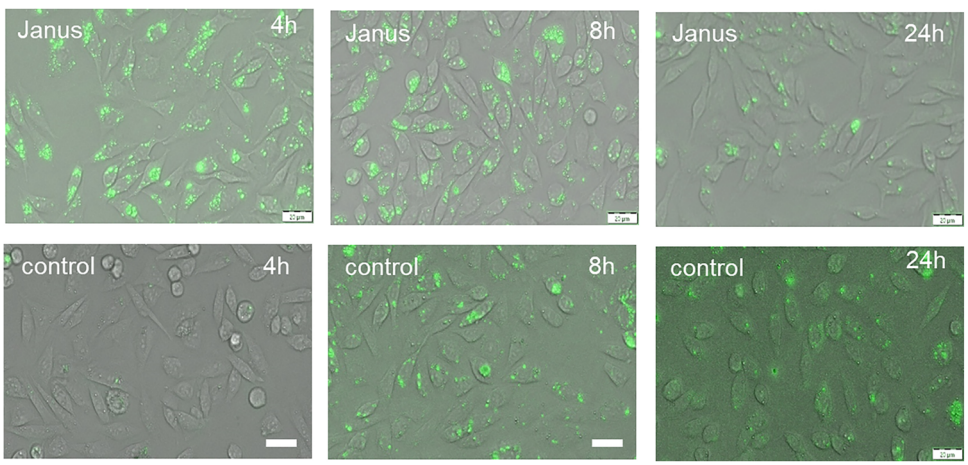

Fig. 5 Enhanced membrane attachment of Janus nanoparticles as compared to control nanoparticles with isotropic decyl functionalization. Cells are incubated with nanoparticles for 4 h/8 h/24 h, and then, the washed cells are used for imaging under bright field or fluorescence mode; merged images are shown here. Results show that Janus nanoparticles can label cells within 4 h but 8 h is required for control nanoparticles.

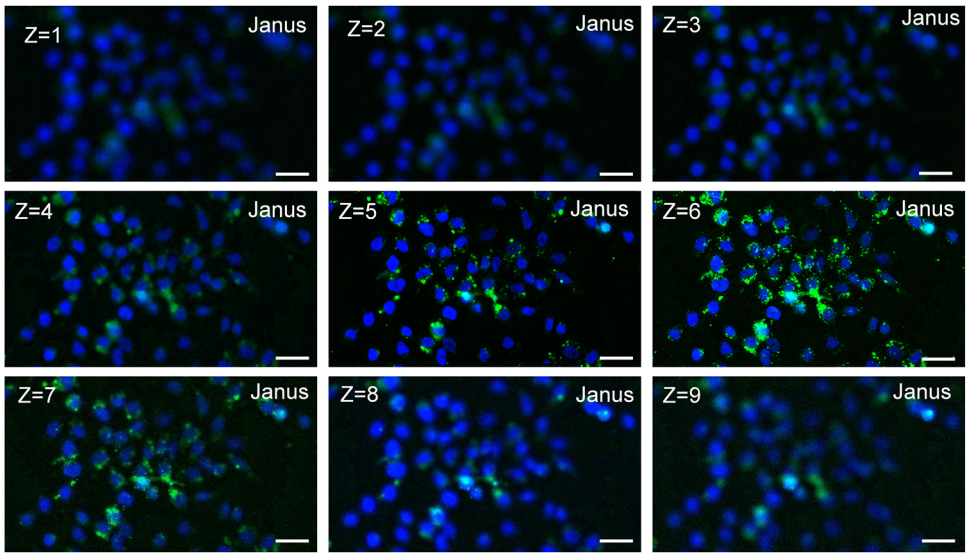

Fig. 6 *Z* stacking images of Janus nanoparticles and nuclear probe-labelled CHO cells. Images are captured at different *Z* planes (top to bottom with consecutive *Z* axis slices of 3.45 micrometers starting from *Z*1 to *Z*9). Green colour represents nanoparticles, and blue colour represents the nuclear probe. Results show that nuclear probe and nanoparticles are present at different *Z* planes. Scale bars are 20 μm.

property can be used for magnetic cell separation applications without appreciable cytotoxicity, provided a lower dose of nanoparticle is used (SI, Fig. S11). However, at higher doses, Janus nanoparticles appear toxic, as expected due to their reported membrane disruption properties.[5,6]

Based on these observations, we proposed a mechanism of enhanced particle–particle interactions due to the Janus structure, leading to poor colloidal stability and extended attachment to the cell membrane (Fig. 7). Janus nanoparticles use their decyl groups for binding with another Janus nanoparticle or the cell membrane. The presence of decyl groups on one side induces surfactant-like characteristics, leading to nanoparticle assembly *via* decyl groups or attachment to the cell membrane. In contrast, isotropic decyl functionalization in the control leads to poor decyl–decyl interactions, resulting in poor particle assembly and poor interactions with the cell membrane. Increased decyl density at the nanoparticle surface (control b) can increase particle–particle interactions, but such interactions lead to the formation of large particle aggregates (and precipitation) that limit their interaction with the cell

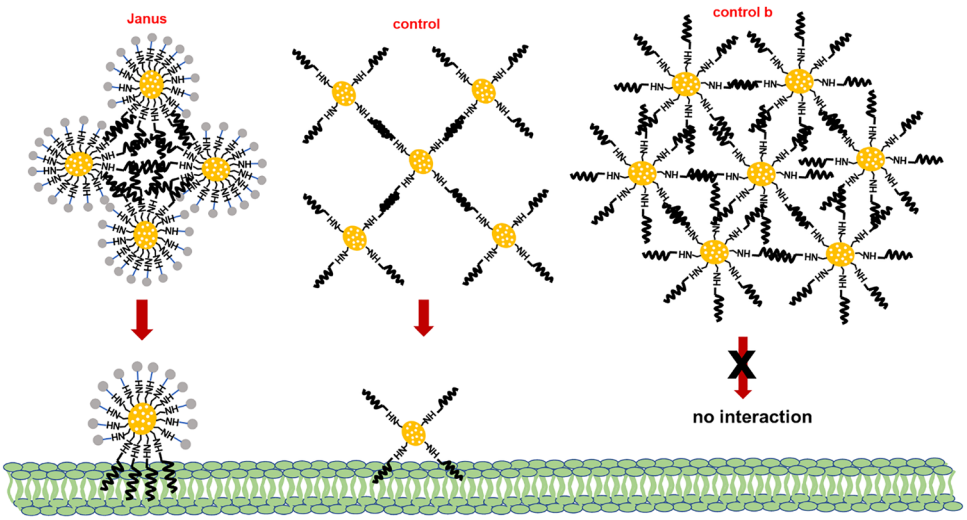

Fig. 7 Proposed mechanism of the self-assembly of Janus nanoparticles using decyl groups and their binding with the cell membrane through decyl groups. Presence of decyl groups at one side induces the surfactant-like nature that leads to modular colloidal assembly *via* decyl groups and decyl-based attachment to cell membrane *via* assembly dissociation. However, isotropically functionalized control nanoparticles with lowers decyl density at surface leads to poor decyl-decyl interaction, poor particle–particle interaction and poor interaction with cell membrane. In contrast, isotropic functionalization with higher decyls (control b) leads to stronger decyl-decyl interaction that leads to 3D particle network that induce particle precipitation before interaction with cell membrane.

membrane. This result further suggests that a Janus structure with modular nanoparticle-nanoparticle interactions is critical, enabling the formation of reversible colloidal aggregates as dispersed form, which disassemble during binding with the cell membrane.

Conclusion

We showed that functionalization of hydrophobic molecules on one side of the nanoparticle surface can enhance their interaction with the cell membrane. We found that this Janus structure induces nanoparticle-nanoparticle interactions *via* the decyl groups, which decreases their colloidal stability and directs the attachment to the lipophilic cell membrane. A comparative study shows that these Janus nanoparticles can label the cell membrane faster than the respective symmetric nanoparticles and remain at the cell membrane for longer times. These results show that the Janus nanostructures offer different physical properties compared to conventionally used isotropically functionalized nanoparticles, thereby inducing distinct interactions with the biological interface.

Conflicts of interest

The authors declare no competing financial interests.

Data availability

The data that support the findings of this study are available in the supplementary information (SI). Data not included in the manuscript are available from the corresponding author upon reasonable request. Supplementary information: procedures for cell uptake mechanism study and cell sample preparation for SEM, summary of the reported anisotropic functionalization-based Janus nanoparticles with unique biomedical applications, evidence of accessibility of one side of the silica particles when present as a stabilizer of wax microemulsion, additional material characterization data and additional control experimental data. This material is available *via* the Internet. See DOI: **https://doi.org/10.1039/d5cp02633d**.

Acknowledgements

NRJ acknowledges DST-SERB (CRG/2023/000432), Government of India, for the financial assistance. PG acknowledges the UGC, Government of India, for providing a research fellowship.

References

1 J. Zhang, B. A. Grzybowski and S. Granick, *Langmuir*, 2017, **33**, 6964–6977.
2 D. Jishkariani, Y. Wu, D. Wang, Y. Liu, A. Van Blaaderen and C. B. Murray, *ACS Nano*, 2017, **11**, 7958–7966.
3 R. Kadam, J. Ghawali, M. Waespy, M. Maas and K. Rezwan, *Nanoscale*, 2020, **12**, 18938–18949.
4 M. Hao, Y. Chen, J. Leisen, T. J. Whitworth and Y. Xia, *J. Am. Chem. Soc.*, 2025, **147**(15), 12973–12981.
5 K. Lee and Y. Yu, *Langmuir*, 2018, **34**, 12387–12393.
6 D. Nguyen, J. Wu, P. Corrigan and Y. Li, *Nanoscale*, 2023, **15**, 16112–16130.
7 J. T. Wiemann, D. Nguyen, S. Bhattacharyya, Y. Li and Y. Yu, *ACS Appl. Nano Mater.*, 2023, **6**, 20398–20409.
8 D. Nguyen, S. Bhattacharyya, H. Richman, Y. Yu and Y. Li, *Nano Lett.*, 2024, **24**(49), 15886–15895.
9 W. Liu, W. Wang, X. Dong and Y. Sun, *ACS Appl. Mater. Interfaces*, 2020, **12**, 12618–12628.
10 M. Žiemytė, A. Escudero, P. Díez, M. D. Ferrer, J. R. Murguía, V. Martí-Centelles, A. Mira and R. Martínez-Máñez, *Chem. Mater.*, 2023, **35**, 4412–4426.
11 W. Chen, R. Jiang, X. Sun, S. Chen, X. Liu, M. Fu, X. Yan and X. Ma, *Chem. Mater.*, 2022, **34**, 7543–7552.
12 W. Cao, Y. Liu, P. Ran, J. He, S. Xie, J. Weng and X. Li, *ACS Appl. Mater. Interfaces*, 2021, **13**, 58411–58421.
13 K. Debnath, S. Pal and N. R. Jana, *Acc. Chem. Res.*, 2021, **54**(14), 2916–2927.
14 A. Chakraborty and N. R. Jana, *J. Phys. Chem. Lett.*, 2015, **6**, 3688–3697.
15 S. Mandal and N. R. Jana, *J. Phys. Chem. C*, 2017, **121**, 23727–23735.
16 R. Ray, S. Pal, S. Das and N. R. Jana, *ACS Appl. Mater. Interfaces*, 2024, **16**, 15819–15831.
17 A. Sinha and N. R. Jana, *Eur. J. Inorg. Chem.*, 2012, 4470–4478.
18 P. Garai, S. Ghosh and N. R. Jana, *ACS Appl. Nano Mater.*, 2024, **7**, 12207–12213.
19 S. Basiruddin, A. R. Maity and N. R. Jana, *RSC Adv.*, 2012, **2**, 11915–11921.
20 J. Wu and G. H. Ma, *Small*, 2016, **12**, 4633–4648.
21 R. Hakanson, L.-I. Larsson and F. Sundler, *Histochemistry*, 1974, **39**, 15–23.